

Nuclear Shadowing and the Optics of Hadronic Fluctuations¹

G. Piller^(a), M. Vanttinen^(a), L. Mankiewicz^(a,b) and W. Weise^(a)

(a) Physik-Department, Technische Universität München, D-85747 Garching, Germany

(b) N. Copernicus Astronomical Center, ul. Bartycka 18, PL-00-716 Warsaw, Poland

Abstract

A coordinate space description of shadowing in deep-inelastic lepton-nucleus scattering is presented. The picture in the laboratory frame is that of quark-gluon fluctuations of the high-energy virtual photon, propagating coherently over large light-cone distances in the nuclear medium. We discuss the detailed dependence of the coherence effects on the invariant mass of the fluctuation. We comment on the issue of possible saturation in the shadowing effects at very small Bjorken- x .

¹Work supported in part by BMBF

1 Introduction: shadowing, diffraction and coherence length

High precision data on shadowing effects in deep-inelastic lepton-nucleus scattering have become available from measurements at CERN (NMC) and FNAL (E665) (for recent reviews see e.g. [1, 2, 3]). Shadowing appears at small values of the Bjorken variable, $x = Q^2/(2M\nu) < 0.1$, as a significant reduction of nuclear structure functions F_2^A compared to the free nucleon one ($q^\mu = (\nu, \mathbf{q})$ is the four-momentum of the exchanged virtual photon with $Q^2 = -q^2$, and M is the nucleon mass).

A closely related process, diffractive photo- and leptonproduction of hadrons from free nucleons, has been investigated in great detail lately at the HERA collider (for a review see e.g. [5]). The connection between shadowing and diffraction has been observed already in Ref.[6]: both processes are driven by the scattering of hadronic components present in the interacting high-energy (virtual) photon. While diffraction reveals the mass spectrum of these hadronic fluctuations, shadowing is a direct measure of their coherent interaction with the nuclear medium. Nuclear shadowing in deep-inelastic lepton scattering can therefore be viewed as the *optics of hadronic (quark-antiquark plus gluon) components of the photon in the nuclear medium*. It provides a tool for investigating the hadronic structure and properties of high-energy (virtual) photons.

For the following discussion we choose the laboratory frame, where the target is at rest, and take the photon momentum \mathbf{q} in the \hat{z} -direction. The nuclear structure function F_2^A , or equivalently, the photon-nucleus cross section $\sigma_{\gamma^*A} = (4\pi^2\alpha/Q^2)A F_2^A$ can be separated into a piece which accounts for the incoherent scattering from individual nucleons, and a correction due to the coherent interaction with several nucleons, $\sigma_{\gamma^*A} = A\sigma_{\gamma^*N} + \delta\sigma_{\gamma^*A}$. The dominant contribution to coherent multiple scattering is described by the well known relation [6, 7]:

$$\begin{aligned} \delta\sigma_{\gamma^*A} = & -8\pi \int_{4m_\pi^2}^{W^2} dM_X^2 \int d^2b \int_{-\infty}^{+\infty} dz_1 \int_{z_1}^{+\infty} dz_2 \rho_A^{(2)}(\mathbf{b}, z_1, z_2) \cos[(z_1 - z_2)/\lambda_X] \\ & \times \left. \frac{d^2\sigma_{\gamma^*N}^{diff}}{dM_X^2 dt} \right|_{t \approx 0} \exp \left[-\frac{\sigma_{XN}}{2} \int_{z_1}^{z_2} dz \rho_A(\mathbf{b}, z) \right]. \end{aligned} \quad (1)$$

A state X with invariant mass M_X is produced diffractively in the process $\gamma^*N \rightarrow XN$, with the nucleon located at (\mathbf{b}, z_1) . The upper limit of M_X is determined by the available γ^*N center-of-mass energy W . The hadronic excitation propagates at fixed impact parameter \mathbf{b} and scatters from a second nucleon at z_2 . The underlying basic mechanism, i.e. diffractive production from a single nucleon, is described by the cross section $d^2\sigma_{\gamma^*N}^{diff}/dM_X^2 dt$ taken in the forward direction with $t = (p - p')^2 \approx 0$, where p and p' are the four-momenta of the active nucleon before and after the diffractive interaction. The nuclear two-particle density, $\rho_A^{(2)}(\mathbf{b}, z_1, z_2)$ accounts for the probability to find two nucleons in the target at the same impact parameter. The exponent in (1) approximates additional

interactions of the diffractively produced hadronic states while they propagate from z_1 to z_2 . The strength of these higher order multiple scattering contributions is described by the effective cross section σ_{XN} . Finally, the $\cos [(z_1 - z_2)/\lambda]$ factor implies that only those diffractively produced hadrons which have a longitudinal propagation length (coherence length)

$$\lambda_X = \frac{2\nu}{Q^2 + M_X^2} = \frac{1}{Mx} \left(\frac{Q^2}{Q^2 + M_X^2} \right) \quad (2)$$

larger than the average nucleon-nucleon separation ($d \simeq 2fm$) in the target nucleus, can contribute significantly to coherent multiple scattering.

Shadowing should therefore start as soon as

$$\lambda_X > d \simeq 2 \text{ fm} . \quad (3)$$

From Eq.(2) one finds that at $Q^2 \gg 1 \text{ GeV}^2$ the condition (3) is met at $x \lesssim 0.1$ in accordance with the measured effect. Since λ_X decreases with increasing M_X , low mass excitations with $M_X \lesssim 1 \text{ GeV}$ are relevant for the onset of shadowing. When x decreases far below 0.1, shadowing increases strongly. This behavior is mainly caused by the diffractive production and coherent multiple scattering of hadronic states with masses $M_X > 1 \text{ GeV}$. At $x \ll 0.1$ it is also the energy dependence of the diffractive production cross section and of the hadron-nucleon cross section σ_{XN} which influences the x -dependence of shadowing.

To illustrate this behavior, consider the shadowing ratio $R_A = \sigma_{\gamma^*A}/A\sigma_{\gamma^*N} = 1 - \delta\sigma_{\gamma^*A}/A\sigma_{\gamma^*N}$, parametrized as:

$$R_A - 1 = -c \left(\frac{1}{x} \right)^\epsilon , \quad (4)$$

with a constant c at small Q^2 where data are actually taken, and a characteristic exponent ϵ . At asymptotically large energies Regge phenomenology suggests $\epsilon \simeq 0.1$ [8, 9].² In Fig.1 we show the quantity

$$\log(1 - R_A) = \log c - \epsilon \log x, \quad (5)$$

plotted versus $\log x$ in comparison with data taken on Pb at small Q^2 . This plot confirms that, for $x < 3 \cdot 10^{-3}$, the shadowing effect indeed approaches the high-energy behavior expected from the Regge limit of diffractive production. Deviations from this asymptotic behavior at larger values of x indicate how shadowing gradually builds up as the coherence length $\lambda_X \propto x^{-1}$ starts to exceed nuclear length scales for diffractively produced states of low mass. At sufficiently high energy or small x , the coherence length becomes comparable

² At the typical average center of mass energies $\overline{W} < 25 \text{ GeV}$ used in experiments at CERN and FNAL, a somewhat stronger energy dependence is expected through the kinematic restriction to diffractively produced hadronic states with masses $M_X < W$.

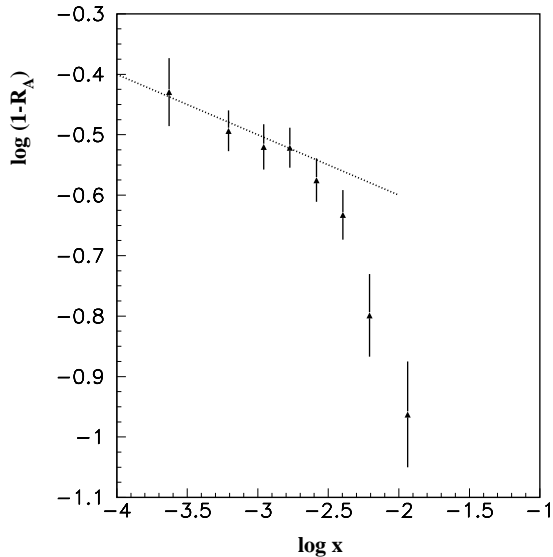


Figure 1: The quantity $\log(1 - R_A)$ as a function of $\log x$ for data taken on Pb [10]. The dashed line corresponds to the asymptotic energy dependence (5) with $\varepsilon = 0.1$.

to nuclear dimensions even for heavy hadronic intermediate states. Then shadowing starts to approach its asymptotic high-energy behavior.

Note that this asymptotic behavior of shadowing sets in when the coherence lengths λ_X of low mass hadronic fluctuations exceed by far the diameter of the nucleus. For example, at $x = 3 \cdot 10^{-3}$ and $Q^2 \simeq 0.7 \text{ GeV}^2$ which corresponds to the onset of the asymptotic behavior in Fig.1, the ρ meson coherence length becomes $\lambda_\rho \simeq 36 \text{ fm}$. The influence of the nuclear size on shadowing is not apparent, and we wish to understand why this is so.

In the following we present a detailed analysis of the role played by characteristic length scales of nuclei in high energy deep-inelastic scattering. In Section 2 we recall the basic features of nucleon and nuclear structure functions in coordinate space. The influence of nuclear scales on the coherent interaction of hadronic states present in the diffractive mass spectrum of the photon is discussed in Section 3.

2 Structure functions in coordinate space

The space-time evolution of nuclear deep-inelastic scattering is viewed most instructively in coordinate space [11, 12] where one can directly compare the characteristic distances

involved in deep-inelastic scattering with scales provided by the nuclear target.

The coordinate-space structure function \mathcal{F}_2 is related to the momentum-space structure function F_2 by:

$$\mathcal{F}_2(l, Q^2) = \int_0^1 \frac{dx}{x} F_2(x, Q^2) \sin(lMx). \quad (6)$$

In the laboratory frame with the \hat{z} -axis along the direction of the incident photon momentum, the Fourier transform (6) projects out contributions from the light-cone, i.e. from time and space intervals along the direction of the photon. We have $t + z = 2l$, and the longitudinal distances involved in the process are $z \simeq t \simeq l$.

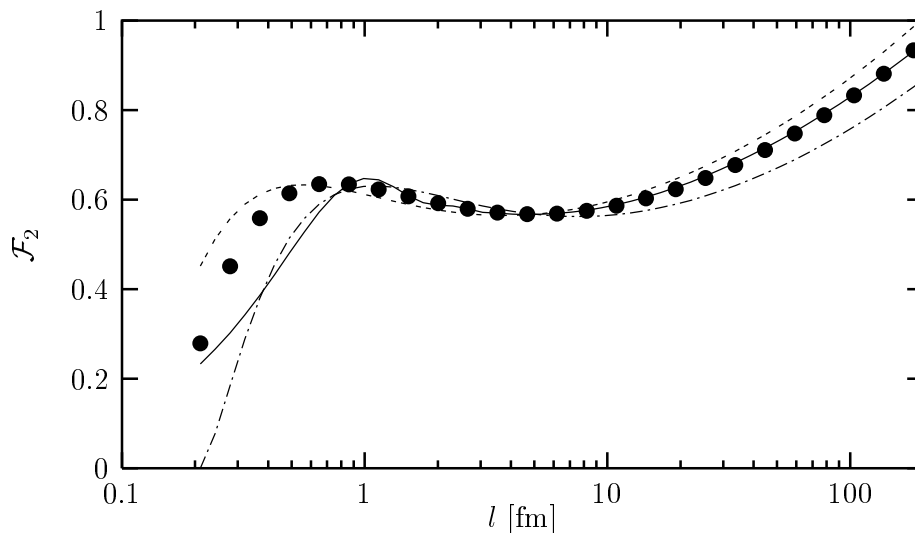


Figure 2: Full line: empirical proton structure function \mathcal{F}_2 in coordinate space for $Q^2 = 2.25 \text{ GeV}^2$ as obtained from the parametrization of Ref.[13]. The full dots correspond to the approximate relation $\mathcal{F}_2(l) \sim F_2(x = 1/(1.5 Ml))$. The dashed and dash-dotted curves correspond to $F_2(x = 1/(2Ml))$ and $F_2(x = 1/(Ml))$, respectively. The approximate coordinate-space distributions are normalized to the exact result at $l = 5 \text{ fm}$.

We show in Fig.2 the proton structure function \mathcal{F}_2 at $Q^2 = 2.25 \text{ GeV}^2$ as obtained from the parametrization of Ref.[13]. One observes that \mathcal{F}_2 rises at small l , develops a plateau at $l \simeq 1 \text{ fm}$, and increases further at large l . At $l < 1 \text{ fm}$ \mathcal{F}_2 is determined by average properties of the corresponding momentum-space structure function F_2 , as expressed by its first few moments [14, 15]. For example, the derivative of \mathcal{F}_2 at $l = 0$ reflects the fraction of the nucleon light-cone momentum carried by quarks. At large distances, $l > 2 \text{ fm}$, \mathcal{F}_2 is governed by the small- x part of F_2 and $l \sim 1/Mx$. As an example, we find approximately $\mathcal{F}_2(l) \sim F_2(x = 1/(1.5 Ml))$ for $Q^2 = 0.5 - 6 \text{ GeV}^2$ as illustrated in Fig.2.

Evidently, the interacting photon-nucleon system at high energy stretches over distances

very large compared to what one usually associates with the "size" of the nucleon. The fact that \mathcal{F}_2 extends over such large distances has a natural interpretation in the laboratory frame: at correlation lengths l much larger than the nucleon size, \mathcal{F}_2 reflects primarily the partonic structure of the interacting photon.

Consider now deep-inelastic scattering from nuclei. The gross features of the observed nuclear effects can be interpreted in a surprisingly simple way when considered in coordinate-space. Two different kinematic regions can be distinguished immediately:

- At distances $l < d$, smaller than the average spacing between two nucleons, $d \sim 2$ fm, the virtual photon interacts incoherently with the constituents bound in the target nucleus.
- At larger distances, $l > d$, several nucleons can participate in the interaction. Deviations of nuclear structure functions from the one of the free nucleon are then expected to come from coherent scattering on at least two nucleons.

Fig.3 shows the ratio of the calcium and free nucleon coordinate-space structure functions, $\mathcal{R}_{F_2} = \mathcal{F}_2^{Ca} / \mathcal{F}_2^N$, as obtained from a fit to empirical nuclear momentum-space structure functions [12]. One observes a clear separation of nuclear effects at small and large distances l . At $l > 2$ fm a strong depletion of the nuclear structure function is found: the virtual photon behaves like a beam of quarks and gluons which scatters coherently from several nucleons in the target causing nuclear shadowing. On the other hand, at $l < 2$ fm nuclear effects are small, indicating that the intrinsic structure of bound nucleons is not much changed in the nuclear environment.

3 Shadowing and nuclear scales

While the average separation of nucleons in nuclei evidently plays a prominent role in the nuclear structure functions, the size of the target nucleus itself seems not to be important: shadowing continues to increase for distances much larger than the nuclear diameter.

The reason for this behavior is found in the fact that the interacting virtual photon couples to a spectrum of hadronic fluctuations which come with different propagation lengths. To investigate this issue further we consider in the following the coordinate-space representation of the shadowing correction $\delta F_2^A = F_2^A - F_2^N$:

$$\delta \mathcal{F}_2^A(l, Q^2) = \int_0^1 \frac{dx}{x} \delta F_2^A(x, Q^2) \sin(lMx). \quad (7)$$

We are interested in the influence of the invariant mass M_X of the diffractively produced hadronic states, as it appears in the coherence length (2). For this purpose, consider first a simple ansatz for the diffractive production cross section which determines the shadowing

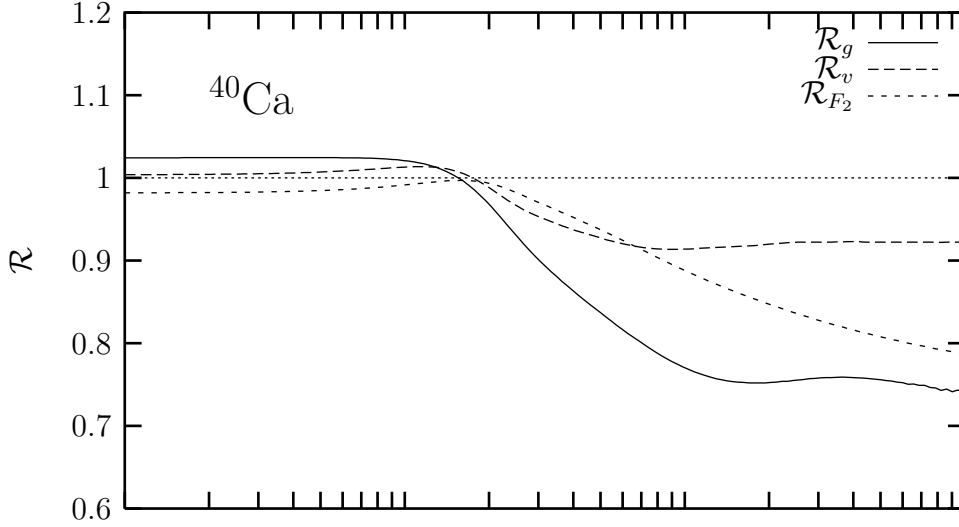


Figure 3: Coordinate-space ratio $\mathcal{R}_{F_2} = \mathcal{F}_2^{Ca} / \mathcal{F}_2^N$ at $Q^2 = 4 \text{ GeV}^2$ for the F_2 structure function of ^{40}Ca as taken from Ref.[12]. Also shown are the ratios for the gluon distributions, \mathcal{R}_g and the valence-quark distributions, \mathcal{R}_v , as discussed in [12]. Note that the nucleon structure functions are normalized per nucleon.

correction in Eq.(1). Suppose that a single, "vector meson" - like state $X = V$ with invariant mass m_V contributes, and that its diffractive production cross-section has the form suggested by vector meson dominance [16]:

$$\left. \frac{d^2 \sigma_{\gamma^* N}^{diff}}{dM_X^2 dt} \right|_{t \approx 0} = \frac{\alpha}{4} \frac{m_V^2 \sigma_{VN}^2}{(m_V^2 + Q^2)^2} \left(\frac{m_V}{g_V} \right)^2 \delta(m_V^2 - M_X^2). \quad (8)$$

In this schematic discussion we use a constant hadron-nucleon cross section, say $\sigma_{VN} \approx 20 \text{ mb}$, and assume that the dimensionless coupling g_V scales roughly with m_V .³ The two-body nuclear density in (1) is expressed as a product of one-body densities multiplied with a nucleon-nucleon correlation function, $\rho_A^{(2)}(\mathbf{b}, z_1, z_2) = \rho_A(\mathbf{b}, z_1) \rho_A(\mathbf{b}, z_2) C(z_1 - z_2)$. The one-body densities $\rho_A(\mathbf{b}, z_1)$ are parametrized by a square well, normalized to the nuclear mass number A . For the correlation function we take a simple step function $C(z) = K \Theta(|z| - z_0)$ with $z_0 = 0.8 \text{ fm}$ [17] and K fixed by the normalization $\int d^3 r_1 d^3 r_2 \rho(\mathbf{r}_1, \mathbf{r}_2) = A^2$.

Fig.4 shows the shadowing correction $\delta \mathcal{F}_2^A$ in coordinate space for ^{12}C at $Q^2 = 4 \text{ GeV}^2$ using different values for the invariant mass m_V of the interacting hadronic state. The onset of shadowing, as well as its saturation at large distances l , shows a significant dependence on m_V . This can easily be explained by recalling Eq.(2). At small values of Bjorken- x the longitudinal interaction length involved in deep-inelastic scattering is given

³For the following discussion the detailed numerical values of σ_{VN} and g_V are actually not relevant.

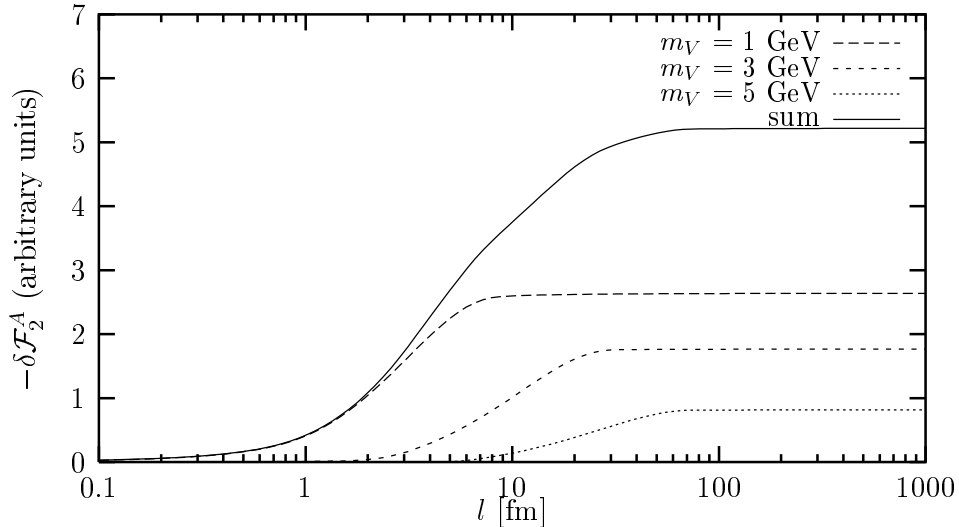


Figure 4: The shadowing correction $\delta\mathcal{F}_2^A$ of Eq.(7) derived from the schematic model (8) for ^{12}C , calculated at $Q^2 = 4 \text{ GeV}^2$ using three different values for the invariant mass m_V of the interacting hadronic state. The solid curve is the sum of all three contributions.

approximately by $l \simeq 2/(3Mx)$ as illustrated in Fig.2. In combination with Eq.(2) one finds that the coherence length λ of a hadronic fluctuation with mass m_V exceeds a given distance Δ when:

$$l > \frac{2\Delta}{3} \left(1 + \frac{m_V^2}{Q^2} \right). \quad (9)$$

The onset of shadowing occurs for distances close to the average nucleon-nucleon separation in nuclei, $\Delta \simeq d \simeq 2 \text{ fm}$. For $m_V \simeq 1 \text{ GeV}$ and $Q^2 \simeq 2 \text{ GeV}^2$ the condition (9) is satisfied at $l \simeq 2 \text{ fm}$. For heavier states Eq.(9) implies larger values of l , in agreement with Fig.4.

At large distances shadowing saturates for each given m_V and approaches a constant value. This behavior is expected once the coherence length gets larger than the nuclear diameter, i.e. $\lambda > 2R_A$. As m_V increases, larger values of l are needed for both the onset and the saturation of shadowing. With $\Delta = 2R_{^{12}\text{C}} \approx 5 \text{ fm}$, the condition (9) reproduces the values of l where saturation is observed in Fig.4.

In summary, the shadowing correction caused by a hadronic state with fixed invariant mass m_V reveals two characteristic nuclear scales, namely the average distance between two nucleons and the nuclear diameter. However, summing over contributions from hadronic fluctuations with different masses masks the role played by the nuclear diameter.

We have just demonstrated these features of coherent nuclear shadowing using a simple

schematic model. This can of course also be verified within a more realistic description of diffractive photon-nucleon scattering. Consider a parametrization [18] for the diffractive cross section, based on Regge phenomenology. The differential production cross section for hadronic states with invariant mass $M_X > 1.2$ GeV is written in factorized form:

$$\left. \frac{d\sigma^{diff}}{dx_{\mathbb{P}} dt} \right|_{t=0} = W^2 \frac{d\sigma^{diff}}{dM_X^2 dt} = \frac{Q^2}{4\pi^2 \alpha} f_{\mathbb{P}/N}(x_{\mathbb{P}}) F_{2\mathbb{P}}(x/x_{\mathbb{P}}, Q^2), \quad (10)$$

where $F_{2\mathbb{P}}$ is commonly interpreted as the ‘‘structure function’’ of the pomeron, and

$$f_{\mathbb{P}/N}(x_{\mathbb{P}}) = \frac{\sigma_{pp}}{16\pi} \frac{1}{x_{\mathbb{P}}^{2\alpha_{\mathbb{P}}-1}} \quad (11)$$

describes its distribution in the nucleon, with $x_{\mathbb{P}} = x \left(1 + \frac{M_X}{Q^2}\right)$ the fraction of the nucleon momentum carried by the pomeron. The intercept of the pomeron is taken to be $\alpha_{\mathbb{P}} = 1.08$ [8]. The proton-proton cross section (due to pomeron exchange) is fixed at $\sigma_{pp} = 40$ mb [18].

The pomeron structure function is split into a quark-antiquark component and a contribution due to triple pomeron exchange, $F_{2\mathbb{P}} = F_{2\mathbb{P}}^{(q\bar{q})} + F_{2\mathbb{P}}^{(3\mathbb{P})}$, where

$$F_{2\mathbb{P}}^{(q\bar{q})} = \frac{8(5 + \lambda_s)\beta_0^2}{3\sigma_{pp}} \frac{N_{sea}Q^2}{Q^2 + Q_0^2} \beta(1 - \beta), \quad (12)$$

$$F_{2\mathbb{P}}^{(3\mathbb{P})} = \frac{g_{3\mathbb{P}}}{\sqrt{\sigma_{pp}}} F_2^{N, sea}(\beta, Q^2). \quad (13)$$

Here $\beta = x/x_{\mathbb{P}}$ is the fraction of the pomeron’s momentum carried by the struck quark. Following [18] we use $\beta_0^2 = 3.4$ GeV⁻², $\lambda_s = 0.5$, $N_{sea} = 0.17$, $Q_0^2 = 0.485$ GeV², and $g_{3\mathbb{P}} = 0.364$ mb^{1/2}. These parameters give a good description of diffractive photoproduction on nuclei, when combined with a cross section $\sigma_{XN} \simeq 20$ mb for the re-scattering of quark-gluon configuration in a multiple scattering expansion. The sea quark contribution $F_2^{N, sea}$ to the nucleon structure function F_2 has been extracted from the parametrizations of Refs.[13].

The contributions of the light vector mesons ρ , ω , and ϕ are described by the vector meson dominance expression (8). The vector meson coupling constants are fixed at $g_{\rho} = 5.0$, $g_{\phi} = 16.3$, and $g_{\omega} = 13.2$. The vector meson-nucleon cross sections are parametrized as: $\sigma_{\rho N} = \sigma_{\omega N} = 13.6s^{\alpha_{\mathbb{P}}-1} + 31.8s^{\alpha_{\mathbb{R}}-1}$ and $\sigma_{\phi N} = 10.0s^{\alpha_{\mathbb{P}}-1} + 1.5s^{\alpha_{\mathbb{R}}-1}$, with $s = W^2$ and $\alpha_{\mathbb{R}} = 0.55$.

With these ingredients data on nuclear shadowing from CERN [4] and FNAL [19] can be reproduced satisfactorily. In Fig.5 we show the resulting shadowing correction δF_2^A in coordinate space, Eq.(7), taken at $Q^2 = 4$ GeV². Contributions from light vector mesons and from hadronic states with intermediate invariant mass, 1.2 GeV $< M_X < 3$ GeV, are displayed separately. We observe the same features as in our previous toy-model results of Fig.4: a specific hadronic state in the diffractive mass spectrum of the photon contributes

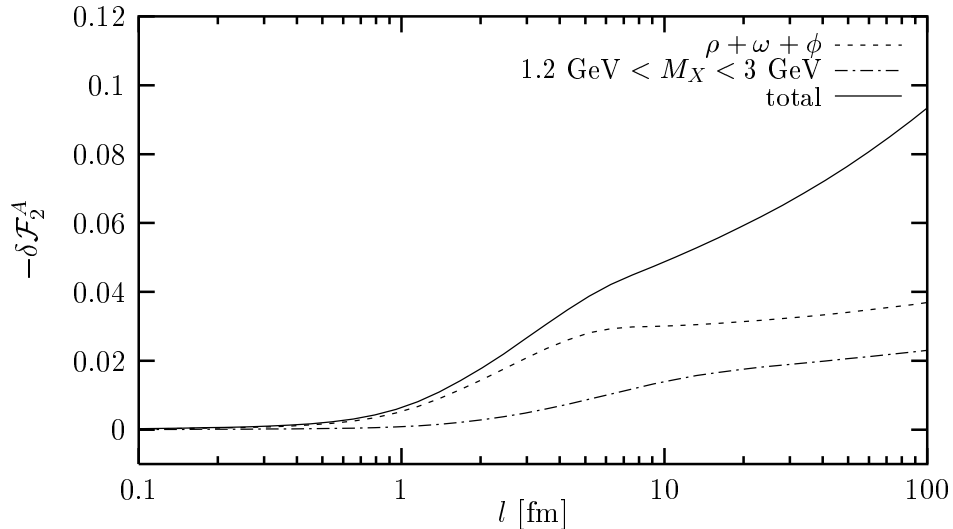


Figure 5: The shadowing correction δF_2^A in coordinate space (7) as obtained from the parametrization of the diffractive production cross of Ref.[18] taken at $Q^2 = 4 \text{ GeV}^2$. Contributions from vector mesons and hadronic states with invariant mass $1.2 \text{ GeV} < M_X < 3 \text{ GeV}$ are shown separately.

significantly to shadowing as soon as its coherence length λ_X exceeds the average nucleon-nucleon distance. Saturation occurs when λ_X becomes larger than the nuclear diameter, or equivalently, for

$$l \gtrsim \frac{4R_A}{3} \left(1 + \frac{M_X^2}{Q^2} \right) \quad (14)$$

Then the weak dependence of shadowing on l reflects the weak energy dependence of the diffractive photon-nucleon cross section. However, after summing over the shadowing corrections from all hadronic states with masses in the entire range $M_X < W$ the saturation condition (14) is dispersed over a broad l -interval and the dependence on the nuclear size gets hidden, leaving the average nucleon-nucleon distance as the only remaining "visible" scale.

4 Summary

Shadowing in deep-inelastic lepton-nucleus scattering at small Bjorken- x can be viewed as an effect related to the coherent propagation of quark-gluon fluctuations of the virtual photon in the nuclear medium, hence the close analogy to notions familiar from wave optics.

This phenomenon is best illustrated in coordinate (rather than momentum) space. At $x \ll 0.1$, the quark-gluon fluctuations extend along the light-cone over distances large compared to the size of the nucleus. The picture in the laboratory frame is that of a "beam" of quark-antiquark pairs and gluons passing through the target nucleus.

The coherence (or propagation) length of each spectral component of this "beam" is governed by its invariant mass. Low mass components propagate over the largest distances and behave as vector mesons. Higher mass components require very high photon energies (at fixed Q^2) or, equivalently, very small Bjorken- x in order to travel over large distances. These components are properly treated within Regge phenomenology, as in high-energy diffractive production.

Each individual spectral component has a distinct shadowing behaviour as a function of the longitudinal distance scale, with the shadowing effect saturating at large distance when propagation length (at given invariant mass) exceeds the nucleon diameter. However, when summing over all (low mass and high mass) fluctuations, we expect that the nuclear radius disappears as a visible parameter and saturation is not reached. This interesting phenomenon should have observable consequences in nuclear structure functions at the smallest possible values of Bjorken- x .

Acknowledgments:

This work was supported in part by KBN grant 2 P03B 011 19.

References

- [1] G. Piller and W. Weise, Phys. Reports 330 (2000) 1.
- [2] D. F. Geesaman, K. Saito and A. W. Thomas, Ann. Rev. Nucl. Part. Sci. 45 (1995) 337.
- [3] M. Arneodo, Phys. Reports 240 (1994) 301.
- [4] NMC, P. Amaudruz et al., Nucl. Phys. B441 (1995) 3.
- [5] H. Abramowicz and A. Caldwell, Rev. Mod. Phys. 71 (1999) 1275.
- [6] V.N. Gribov, Sov. Phys. JETP 30 (1970) 709.
- [7] V.A. Karmanov and L.A. Kondratyuk, JETP Lett. 18 (1973) 266.
- [8] A. Donnachie and P.V. Landshoff, Phys. Lett. B296 (1992) 227.
- [9] P.D.B. Collins, An Introduction to Regge Theory and High-Energy Physics (Cambridge University Press, Cambridge, UK, 1977).
- [10] E665, M.R. Adams et al., Z. Phys. C67 (1995) 403.
- [11] P. Hoyer and M. Vanttinen, Z. Phys. C74 (1997) 113.
- [12] M. Vanttinen, G. Piller, L. Mankiewicz, W. Weise and K.J. Eskola, Eur. Phys. J. A3 (1998) 351.
- [13] H. Abramowicz and A. Levy, hep-ph/9712415.
- [14] L. Mankiewicz and T. Weigl, Phys. Lett. B380 (1996) 134.
- [15] T. Weigl and L. Mankiewicz, Phys. Lett. B389 (1996) 334.
- [16] T.H. Bauer, R.D. Spital, D.R. Yennie and F.M. Pipkin, Rev. Mod. Phys. 50 (1978) 261.
- [17] G.E. Brown, S.O. Bäckmann, E. Oset and W. Weise, Nucl. Phys. A286 (1977) 191.
- [18] W. Melnitchouk and A.W. Thomas, Phys. Lett. B317 (1993) 437.
- [19] E665, M.R. Adams et al., Phys. Rev. Lett. 68 (1992) 3266.